

1-3 Piezoelectric Composite Ferroelectric Materials in Smart Medical Ultrasonic Diagnostic Transducers

Ahthashame Ullaha Khan*

Institute of IT & Computer Science, Afghanistan

**corresponding author*

Keywords: Ultrasonic Transducer, 1-3 Piezoelectric Composite Material, Finite Element Research, ANSYS Finite Element Analysis

Abstract: Piezoelectric ultrasonic transducer is the most important functional device in the field of ultrasound, as an important part of piezoelectric ultrasonic transducer-piezoelectric material, the improvement of its performance plays an important role in promoting the innovation and development of piezoelectric ultrasonic transducers. This article aims to conduct a finite element study based on the 1-3 piezoelectric composite ferroelectric material of the smart medical ultrasonic diagnostic transducer. In this article, the working principle and function of the ultrasonic transducer are explained first. The ultrasonic transducer is classified, and the FEM analysis of the 1-3 piezoelectric composite ferroelectric material and the ANSYS FEM analysis method are introduced. The influence of PZT volume fraction, aspect ratio and the number of primitives on the finite element model of the 1-3 spherical-crown piezoelectric composite is mainly discussed, and then verified by experiments and ANSYS performance analysis of ultrasonic diagnostic transducers. The research results show that the thickness electromechanical coupling factor of the 1-3 piezoelectric composite material is affected by the thickness electromechanical coupling coefficient of the piezoelectric phase material, the volume fraction of the piezoelectric phase, and the width-to-thickness ratio. When the aspect ratio is increased to 0.7, the electromechanical coupling coefficient of the thickness with a volume fraction of 80% is reduced by 79%. The electromechanical coupling coefficient of the thickness with a volume fraction of 60% is reduced by 73%, and the electromechanical coupling coefficient of the thickness with a volume fraction of 20% is reduced by 68%.

1. Introduction

Ultrasound specialty came into being in the early days of the last era. It is a comprehensive discipline developed from traditional classical acoustics as a foundation and incorporating a variety of professional theories. Ultra-acoustic technology has not only been widely used in the traditional

industrial and agricultural fields, but also has been widely used in the fields of medicine, national defense, biology and aerospace. Ultrasonic is generally an in-depth study of various issues such as the formation, transmission, reception, data processing and related effects of ultrasound in various media. It is the emergence of ultrasound transducers that has brought the research methods of ultrasound to a new stage. The transducer, as its name implies, is an energy conversion element, which usually refers to the element that performs the mutual conversion of alternating electrical signals and sound waves in the ultrasonic frequency range, thereby generating the function of transmitting and receiving ultrasonic waves. Ultrasonic transducer is the most important functional device in ultrasonic equipment. When ultrasonic waves propagate in media, they can produce many chemical, physical and biological effects. At the same time, ultrasonic waves have many advantages such as strong penetrating power, large information carrying capacity, and good clustering. It is precisely because of the above-mentioned advantages of ultrasound that ultrasonic transducers can be widely used in engineering non-destructive inspection, biomedical inspection, underwater sonar and other fields.

There are quite a few types of ultrasonic transducers, which are classified according to the material used by the transducer and the energy conversion mechanism. Ultrasonic transducers can be divided into magnetos transducers, high-frequency capacitive transducers, high-voltage electric transducers, mechanical transducers and many other categories. Among the transducers in the world, the piezoelectric ultrasonic transducer is the most used and the most complete theoretical research results. 1-3 Piezoelectric composite materials are particularly obvious for the development of new ultrasonic transducers, and the performance of hybrid materials can be modified through application design.

Combined with the research progress at home and abroad, different scholars have made certain explorations in the finite element research of ultrasonic transducers and ferroelectric materials: Dudley N J studied A simple "connector test" was studied to diagnose the operation of the elements in the ultrasonic transducer array, and has been applied to the phased array, the purpose is to further adjust the multi-line transducer array test [1]. Westerway SC studied Australia's findings on medical ultrasound disinfection and hygiene practices, and the results emphasized that there is an urgent need to update medical ultrasound infection prevention and control guidelines [2]. Hager PA proposed a configurable beam former, and proved that the entire 3-D delay and summing beamforming can be fully digitalized on a single chip, without the need for off-chip memory [3]. Lee W gave an overview of medical ultrasound imaging transducers, and detailed structural components of typical transducers. Including the active layer, the acoustic matching layer, the backing block, the acoustic lens and the notch [4]. Lei M conducted a theoretical study, obtained the corresponding dielectric constant, tunability and electric field distribution from finite element analysis, and analyzed the relationship between these parameters. Also by constructing a series of models of different dielectrics, the influence of the relative relationship between the dielectric constants of ferroelectrics and dielectrics on the overall dielectric properties is analyzed [5]. Wang D used the finite element method to simulate BaTiO₃-based nano-scale piezoelectric energy harvester with the same material size. And compared it with the corresponding results of the ferroelectric energy harvester, in which the new advantage strategy is proved [6]. Lange S introduced the so-called aggregation method to study the behavior of macro-polycrystalline ferroelectric materials at the global material point without any discretization scheme. It extends from the condensation method to the behavior of ferromagnetic and ferrous materials [7]. Avakian A introduced the construction model of nonlinear multi-field behavior and the realization of finite element. A nonlinear material model describing the electric or electric ferromagnetic behavior of magnets is

introduced. The polarization of the ferroelectric phase, the magnetization of the ferromagnetic phase and the magnetos phase are simulated respectively, and the resulting influence is analyzed [8]. However, these scholars did not explore the ultrasonic transducer based on the finite element analysis method, but only made a unilateral elaboration on it.

The key points of research and innovation of this article are as follows: (1) This article gives a comprehensive introduction to the ultrasonic transducer, and gives the finite element analysis of the 1-3 piezoelectric composite ferroelectric material; (2) The effect and far-reaching influence of PZT volume fraction, aspect ratio and the number of primitives on the finite element modeling of 1-3 spherical crown piezoelectric composites are discussed. Then it was verified by experiment and ANSYS performance analysis of ultrasonic diagnostic transducer.

2. Finite Element Research Method Based on 1-3 Piezoelectric Composite Ferroelectric Materials in Smart Medical Ultrasonic Diagnostic Transducers

2.1. Smart Medical Ultrasound Diagnosis Transducer

The principle of ultrasonic transducer is piezoelectric ceramics that resonate at the ultrasonic frequency. Due to the piezoelectric effect of various materials, electrical signals are converted into machine vibrations. The working principle of medical ultrasonic transducer (ultrasound probe) is also roughly the same, it generally contains a set of mechanical vibration control system [9]. When the transducer is used as a transmitter, the power oscillation information brought by the excitation power supply will cause the charge and magnetism of the electric energy storage device in the transducer to change. These changes use an action effect to form a driving force for the mechanical vibration system in the transducer and make it enter an oscillation state. In turn, the medium in contact with the mechanical oscillation control system of the transducer is caused to oscillate and radiate sound waves to the center of the medium [10]. Through some physical effects, the charge or magnetism in the energy storage element of the transducer has formed a certain change, and this leads to the formation of a voltage and current corresponding to the sound signal at the electrical output end of the transducer [11].

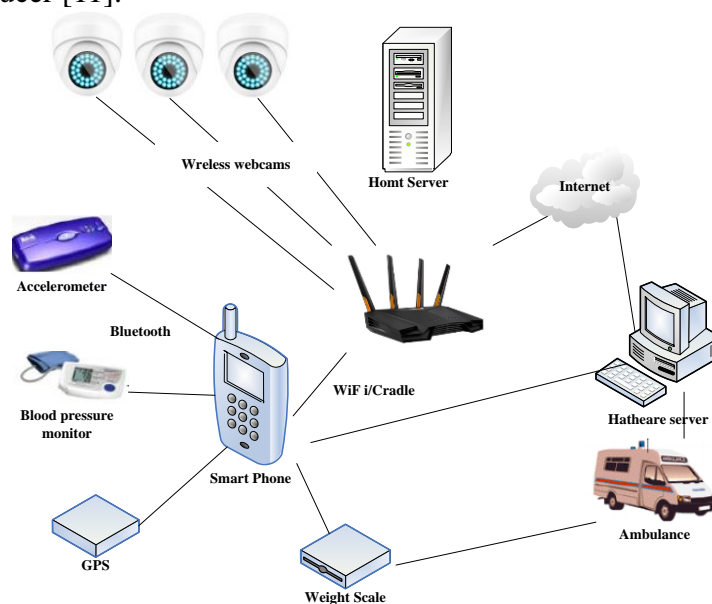


Figure 1. Smart home medical system for remote monitoring

Among them, the medical ultrasonic transducer (ultrasound probe) is one of the main parts of the medical ultrasonic instrument system, and it is in a very critical position in the development of new medical instruments and equipment and in the process of medical research [12]. Figure 1 is a smart home medical system for remote monitoring. In ultrasound therapy, it is first necessary to send ultrasound into the body, and then receive the reflected echo of the tissue structure information in the body. The equipment with the function of handshaking is the medical ultrasonic transducer. With it realizes various electro-acoustic and acoustic-electric transformations, the characteristic state of the transducer will be directly related to the operating characteristics of the medical ultrasonic device [13].

At the same time, the ultrasonic transducer also involves transforming AC signals into sound information in the ultrasonic signal spectrum area and transforming sound information and external sound fields into electric signals, also known as ultrasonic sensors. It also has some basic characteristics and technical parameters, including width, resonance frequency, sound quality factor, coupling coefficient, frequency characteristics and sound pressure level, directivity, etc. [14].

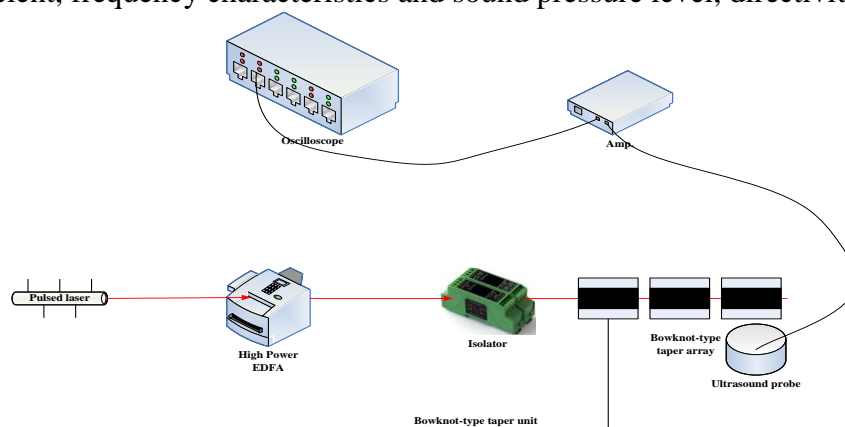


Figure 2. Device diagram of ultrasonic transducer

Ultrasonic transducers usually have the following basic structures. As shown in Figure 2, it is the installation diagram of the ultrasonic transducer. According to the mechanism of electric energy change, it should be divided into electromagnetic ultrasonic transducer, piezoelectric transducer, magnetos transducer, electrostatic transducer and so on. According to the way of vibration, it can be classified into a vertical direction (thickness) vibration sensor, a bending vibration sensor, and a shear vibration transducer. According to the work and transmission medium of the transducer, it can be divided into gas-mediated ultrasonic transducer, liquid conduction transducer and solid-state mediated ultrasonic transducer [15]. According to the receiving status at work, it can be divided into receiving ultrasonic transducer, output ultrasonic transducer, transmitting and receiving ultrasonic transducer, etc. In addition, according to the requirements of various occasions, there are spherical degree wave ultrasonic medical transducers, plane wave ultrasonic medical transducers. The article is mainly based on the FEM analysis of the 1-3 piezoelectric composite ferroelectric material based on the intelligent medical ultrasonic diagnostic transducer [16].

2.2. Finite Element Analysis Method of 1-3 Piezoelectric Composite Ferroelectric Materials

Since the concept of piezoelectric composite material was put forward, scientists from many countries have carried out large-scale in-depth research on it to explore the equivalent properties of

the material in its various composite methods. The main research and analysis methods of piezoelectric composites include theoretical research, parameter identification research, numerical research and experimental research [17]. Here is a brief introduction to several commonly used analysis methods.

The research methods for macroscopic equivalent characteristics generally include two types: inclusion theory and uniform field theory. The doping theory is based on mechanics. After doping the representative volume unit (cell body) of the 1-3 piezoelectric composite material, start with the constitutive equations of the matrix phase and piezoelectric phase of the 1-3 piezoelectric composite material, and finally determine the phase equivalent characteristics of the composite 1-3 piezoelectric composite material by integrating the performance of each relevant unit. The piezoelectric phase and matrix phase of the 1-3 piezoelectric sensing composite material conform to the constitutive equation:

$$\omega^d = Q^d \varphi^d - k^{dD} K^D \quad (1)$$

$$G^d = k^d \varphi^d + \beta^d K^D \quad (2)$$

Among them, k^{dD} is the constant-stress piezoelectric stress coefficient matrix, φ is the strain matrix, k is the clamping dielectric constant matrix, Formula (5)(6) can be obtained from formula (3)(4).

$$\langle \omega \rangle = \frac{1}{L} \int_L^1 \omega gl = \frac{1}{L} [\int_{L_m}^1 \omega gl + \int_{L_p}^1 \omega gl] \quad (3)$$

$$\langle G \rangle = \frac{1}{l} \int_v^1 G gl = \frac{1}{l} [\int_{L_m}^1 G gl + \int_{L_p}^1 G gl] \quad (4)$$

$$\langle \omega \rangle = l_p \langle \omega^p \rangle + (1 - l_p) \langle \omega^m \rangle \quad (5)$$

$$\langle G \rangle = l_p \langle G^p \rangle + (1 - l_p) \langle G^m \rangle \quad (6)$$

Substituting formula (5)(6) into formula (1)(2) can obtain formula (7)(8).

$$Q^* \varphi^\circ - k^{*D} K^\circ = Q^* \varphi^\circ - k^{mD} K^\circ + l_p (\nabla Q \langle \varphi^d \rangle - \nabla k^D \langle K^p \rangle) \quad (7)$$

$$k^* \varphi^\circ + \beta^* K^\circ = k^m \varphi^\circ + \beta^m K^\circ + l_p (\nabla k \langle \varphi^p \rangle - \nabla \beta \langle K^p \rangle) \quad (8)$$

The relationship between $\langle \varphi^p \rangle$, $\langle K^p \rangle$ and uniform boundary conditions $\langle \varphi^\circ \rangle$, $\langle K^\circ \rangle$ in the formula is two well-known models: Dilute model and Mori-Tanaka model [18].

(a) Dilute model. It assumes that there is no interaction between the two inclusion phases, and according to the uniform field theory, it assumes that the stress field and the electric displacement field of the piezoelectric phase satisfy:

$$\langle \varphi^p \rangle = X \varphi^\circ + Y K^D, \langle K^p \rangle = x \varphi^\circ + y K^D \quad (9)$$

Combining formula (1)(2), substituting formula (9) into formula (5)(6), comparing the coefficients of φ° and K° on both sides, you can get the macroscopic equivalent constant expression of 1-3 piezoelectric composite material.

(b) Mori-Tanaka model. It assumes that a single inclusion is still surrounded by a matrix, but it is subject to the $\langle \varphi^m \rangle$ and $\langle K^m \rangle$ fields. There are:

$$\langle \varphi^p \rangle = M \langle \varphi^m \rangle + N \langle K^m \rangle, \langle K^p \rangle = m \langle \varphi^m \rangle + n \langle K^m \rangle \quad (10)$$

In addition

$$\langle \varphi^\circ \rangle = l_p \langle \varphi^p \rangle + (1 - l_p) \langle \varphi^m \rangle, \langle K^\circ \rangle = l_p \langle K^p \rangle + (1 - l_p) \langle K^m \rangle \quad (11)$$

The meanings of X, Y, x and y in formula (10) are the same as formula (9), combined with the previous algorithm equation, an analytical formula of equivalent constant can be obtained. The solution method of inclusion theory can better reflect the actual situation of the material, and the accuracy of the solution is relatively high, but it also has shortcomings [19]. The calculation and problem-solving of inclusion theory are relatively cumbersome, and sometimes only numerical methods can be used to solve equations.

When developing piezoelectric sensing composite materials (including piezoelectric phase and polymer phase), the Tetrahedral unit is used (the SOLID five piezoelectric unit is used in ANSYS software), the main reason is that the Tetrahedral unit is conducive to the establishment of a three-dimensional piezoelectric structure, and the use of the Tetrahedral unit composition at the same time can easily establish various types of three-dimensional space structures. In a finite element formula, the interpolation function between the displacement field and the electric field is always the same [20]. For an independent finite element, its structural strain V^c can be described as:

$$\{V^c\} = \begin{Bmatrix} \delta_x \\ \delta_y \\ \delta_z \\ \varphi_{yz} \\ \varphi_{xz} \\ \varphi_{xy} \end{Bmatrix} \begin{Bmatrix} \frac{\sigma_u}{\sigma_x} \\ \frac{\sigma_v}{\sigma_y} \\ \frac{\sigma_w}{\sigma_z} \\ \frac{\sigma_v}{\sigma_z} + \frac{\sigma_w}{\sigma_y} \\ \frac{\sigma_u}{\sigma_z} + \frac{\sigma_w}{\sigma_x} \\ \frac{\sigma_u}{\sigma_y} + \frac{\sigma_v}{\sigma_x} \end{Bmatrix} \quad (12)$$

In the finite element formula, the displacements u, v, w can approximately represent the nodal displacements u_i, v_i, w_i and the nodal shape function M_i function:

$$u = \sum_{i=1}^m M_i u_i \quad v = \sum_{i=1}^m M_i v_i \quad w = \sum_{i=1}^m M_i w_i \quad (13)$$

Substituting the above formula into formula (12), we can get

$$\{V^c\} = \begin{Bmatrix} \delta_x \\ \delta_y \\ \delta_z \\ \varphi_{yz} \\ \varphi_{xz} \\ \varphi_{xy} \end{Bmatrix} \begin{Bmatrix} \frac{\sigma \sum_{i=1}^m M_i u_i}{\sigma_x} \\ \frac{\sigma \sum_{i=1}^m M_i v_i}{\sigma_y} \\ \frac{\sigma \sum_{i=1}^m M_i w_i}{\sigma_z} \\ \frac{\sigma \sum_{i=1}^m M_i v_i}{\sigma_z} + \frac{\sigma \sum_{i=1}^m M_i w_i}{\sigma_y} \\ \frac{\sigma \sum_{i=1}^m M_i u_i}{\sigma_z} + \frac{\sigma \sum_{i=1}^m M_i w_i}{\sigma_x} \\ \frac{\sigma \sum_{i=1}^m M_i u_i}{\sigma_y} + \frac{\sigma \sum_{i=1}^m M_i v_i}{\sigma_x} \end{Bmatrix} \quad (14)$$

Because the node movement value has been given, and the manifold function of the node can also be regarded as a function of the coordinate point, the above formula (14) can be written as the shape of the matrix:

$$\{V^c\} = [H_u]\{u^c\} \quad (15)$$

Matrix $[H_u]$ contains the expansion of the displacement field shape function, which can be written as:

$$[H_u] = \begin{bmatrix} [M_x] & 0 & 0 \\ 0 & [M_y] & 0 \\ 0 & 0 & [M_z] \\ 0 & [M_z] & [M_y] \\ [M_z] & 0 & [M_x] \\ [M_y] & [M_x] & 0 \end{bmatrix} \quad (16)$$

In the above formula, $[M_x]$, $[M_y]$, and $[M_z]$ are the shape functions corresponding to each node on the finite element in x, y, and z.

The element stiffness matrix of the finite unit in the electric complex can be obtained by calculating the effective work inside the unit and the reasonable work done by the joint action of the mechanical load of the unit external node and the unit external electric load [21]. For example, it can be described as:

$$\int w\{\sigma V^c\}^K\{K^c\}dW = \{\sigma u^c\}^K\{A^c\} - \int w\{\sigma C^c\}^K\{D^c\}dW = \{\sigma u^c\}^K\{R^c\} \quad (17)$$

Substituting formula (17) into formulas (15) and (16) respectively, we can get:

$$\{\sigma u^c\}^K \int W [H_u]^K [C] [H_u] \{u^c\} + [H_u]^K [c]^K [H_\phi] \{\varphi^c\} dW = \{\sigma u^c\}^K \{A^c\} \quad (18)$$

$$\{\sigma \varphi\}^K \int W [H_\phi]^K [c] [H_u] \{u^c\} + [H_\phi]^K [\varepsilon] [H_\phi] \{\varphi^c\} dW = \{\sigma \varphi^c\}^K \{R^c\} \quad (19)$$

By simplifying the above formula, the element finite element formula can be obtained as:

$$\begin{bmatrix} [Z_{uu}^c] & [Z_{u\phi}^c] \\ [Z_{\phi u}^c] & [Z_{\phi\phi}^c] \end{bmatrix} \begin{Bmatrix} \{u^c\} \\ \{\varphi^c\} \end{Bmatrix} = \begin{Bmatrix} \{A^c\} \\ \{R^c\} \end{Bmatrix} \quad (20)$$

Therefore, as long as the standard conformal function is selected for the element between 4 nodes and 10 nodes, the element stiffness matrix of piezoelectric composite materials can be derived [22].

2.3. Overview of ANSYS Finite Element Analysis Method

ANSYS software system is an universal FEM analysis software system that integrates construction, streamline, electromagnetic, and sound field analysis methods. It is widely used in engineering, scientific research and other fields [23]. ANSYS software realizes multiple functions such as structural analysis, electromagnetic analysis, fluid dynamics analysis, collision analysis, and adaptive mesh analysis [24]. ANSYS also proposes the addition of macro instruction function for parameter design statements, which provides users with secondary development functions. The ANSYS software system has been able to adapt to the requirements of finite element analysis in the general engineering field, so we use the ANSYS software system to analyze the finite element simulation of 1-3 piezoelectric composite materials.

In the process of building simulations for piezoelectric sensing composite materials and transducers using ANSYS finite element method, the general process includes: first simplifying the

test problem, converting it into a simple mathematical model, and then clarifying the material parameters and specific specifications of each phase. Finally, a simple finite element model is formed and divided into grids to ensure the accuracy of the test. Then add electrodes to the set geometric model, provide load and boundary conditions, and then solve it by the established equations. After the calculation is completed, the data and conclusions obtained by the post-processing module are displayed in the form of images and lists [25]. The steps are shown in Figure 3:

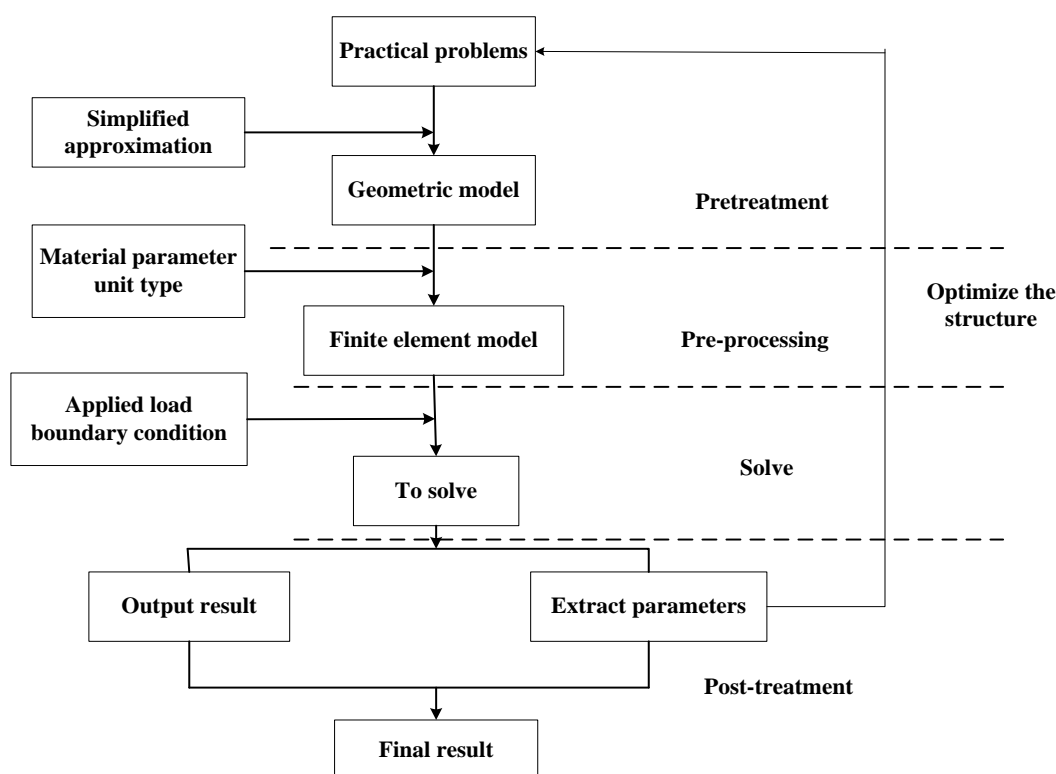


Figure 3. ANSYS analysis flow chart

3. Experimental Results Based on Finite Element Research of 1-3 Piezoelectric Composite Ferroelectric Materials in Smart Medical Ultrasonic Diagnostic Transducers

This article first explores the influence of PZT volume fraction, aspect ratio, and the number of primitives on the finite element model of 1-3 spherical-crown piezoelectric composites. Explore the first six-order natural frequency values of the piezoelectric composite material PZT with different thicknesses of the miniature piezoelectric ultrasonic sensor, and then verify it through experiments and ANSYS results.

3.1. Finite Element Analysis of PZT on Piezoelectric Composites

Figure 4 shows the electromechanical performance curves of the finite element model with different PZT volume fractions. The resonance peaks of all curves are dominated by a single vibration and the resonance peaks are very obvious, which preliminarily proves the accuracy and feasibility of the design process parameters of piezoelectric composite materials. In addition, when the PZT volume fraction increased from 27.0% to 70.6%, the resonant frequency of the

piezoelectric composite material changed slightly in the range of 20k Hz, and the conductance peak at the resonance point increased from 45ms to 186ms, an increase of 350%.

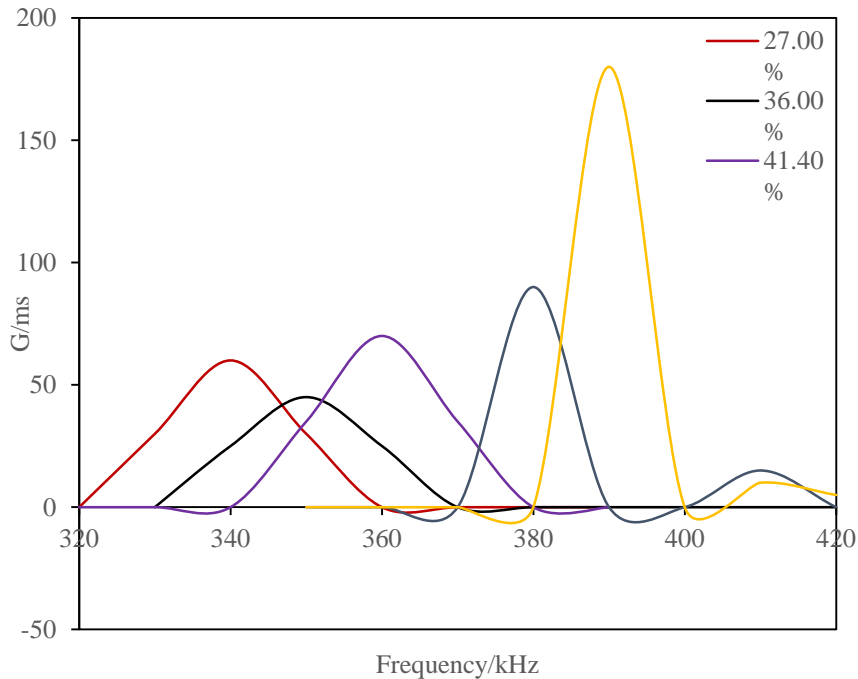


Figure 4. Analysis curve of electromechanical performance of piezoelectric composite

The left picture in Figure 5 is the electromechanical performance analysis diagram of the finite element model with different PZT column aspect ratios. The PZT column aspect ratio has an effect on the resonance frequency of the piezoelectric composite material and the peak value at the resonance point. All electromechanical performance curves have complete and obvious resonance peaks, the vibration mode is dominated by radial vibration, and there are basically no spurious peaks. When the PZT column aspect ratio gradually increases, the resonance frequency of the piezoelectric composite material rises from 350kHz to 470kHz, an increase of 110kHz; in addition, the peak conductance changes from 130ms to 238ms, an increase of 75%.

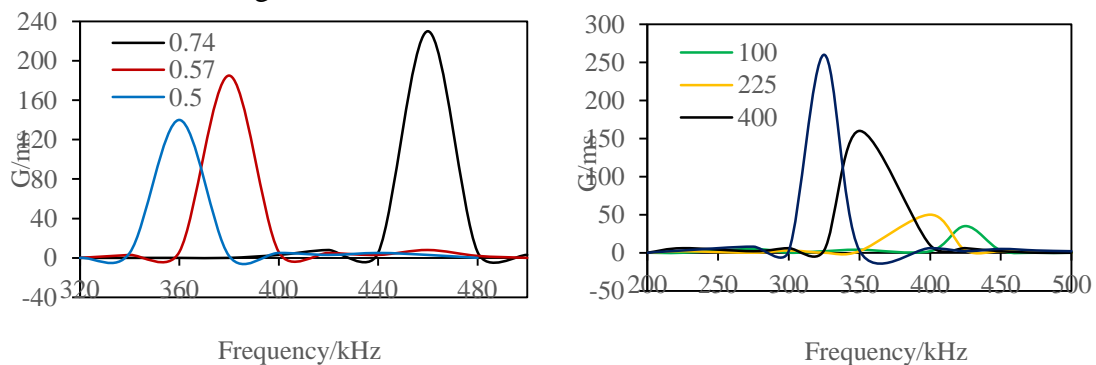


Figure 5. Different PZT electromechanical performance analysis curves

The right picture in Figure 5 is the electromechanical performance curve of the finite element

model of the PZT column element number 1-3 piezoelectric composite ferroelectric material. There is only one resonance peak in all curves 200k Hz-500kHz. When the number of PZT primitives increases from 100 to 900, the resonance frequency of the 1-3 piezoelectric composite ferroelectric material changes in the frequency range of 300kHz-430kHz, and the conductance peak at the resonance point gradually increases as the number of PZT column primitives increases. When the number of PZT primitives is 100, the peak conductance at the resonance point of the piezoelectric composite is 35ms. When the number of PZT primitives is 900, the peak conductance at the resonance point is 265ms, an increase of 230ms.

With high temperature resistant epoxy resin as the matrix phase and PZT-4 piezoelectric ceramics as the functional phase, 1-3 spherical crown piezoelectric composites with different PZT volume fractions were prepared. The dimensions of the five different PZT volume fraction piezoelectric composite materials are all 62mm×62mm, and the spherical cap opening angles are all 39°. Table 1 shows the structural parameters of piezoelectric composite materials:

Table 1. PZT structure parameters

PZT volume fraction	PZT aspect ratio (width/height)	PZT size/mm(length*width*height)	PTZ spacing/mm	Number of PTZ columns
27.0%	0.61	2.4*2.4*4.36	0.4	171
36.0%	0.61	2.4*2.4*4.36	0.9	201
41.4%	0.61	2.4*2.4*4.36	1.6	223
51.8%	0.61	2.4*2.4*4.36	1.9	231
70.6%	0.61	2.4*2.4*4.36	2.3	398

From Table 2, we can find that although the PZT series piezoelectric composite materials are very suitable as piezoelectric devices in transmitting transducers, in fact, the piezoelectric effect of various piezoelectric sensing materials is quite different. Through simulation analysis and comparison, the piezoelectric device with PZT-4 as the transducer has the best effect. The displacement, sound pressure, acceleration, etc. excited by the same part of the same oil and gas pipeline are all larger than other materials. When the same current is applied to the transducer, the axial stress obtained is also larger than that of other materials, followed by PZT-8, while the effect of PZT-5A and PZT-5H is lower than that of PZT-4 and PZT-8.

Table 2. The performance of the four piezoelectric materials as the piezoelectric element of the transducer

Piezoelectric material	Backing height (mm)	H1(mm)	Displacement (mm)	Sound pressure (N/S2)	Acceleration (m/S2)	Stress (N/m2)
PZT-4	320.1	130	0.19202	8.5379E6	2302.1	4.79E8
PZT-8	324.02	130	0.11998	5.4698E6	1459.8	2.98E8
PZT-5A	3140.1	130	0.033986	1.5221E6	408.51	8.49E7
PZT-5H	312.03	130	0.020968	9.4002E5	251.98	5.31E7

Table 3 shows the first six-order natural frequency values of the piezoelectric composite material PZT with different thicknesses of the miniature piezoelectric ultrasonic sensor. It can be seen from the table that the first-order natural frequencies of the structure are all greater than 40K Hz, which meets the frequency requirements of ultrasonic waves. As long as our excitation voltage reaches the

natural frequency value, the sensor can be excited to resonate, and then the ultrasound can be excited.

Table 3. The natural frequencies of each stage of the miniature piezoelectric ultrasonic sensor with different thicknesses of the piezoelectric composite ferroelectric material PTZ

H-PZT(um)	3	5	7	9
First-order natural frequency (Hz)	45002	46023	47003	49013
Second-order natural frequency (Hz)	52988	54002	56002	58001
Third-order natural frequency (Hz)	87701	90062	91987	96005
Fourth-order natural frequency (Hz)	0.12397E+06	0.12601E+06	0.13002E+06	0.12999E+06
Fifth-order natural frequency (Hz)	0.12986E+06	0.13801E+06	0.13997E+06	0.14701E+06
Sixth order natural frequency (Hz)	0.15987E+06	0.16398E+06	0.17008E+06	0.18022E+06

Figure 6 reflects the dependence of the electromechanical coupling coefficient of the research unit of PMN-0.3PT relaxant ferroelectric single crystal and PZT-5H piezoelectric ceramic on G when filling materials with different stiffness coefficients.

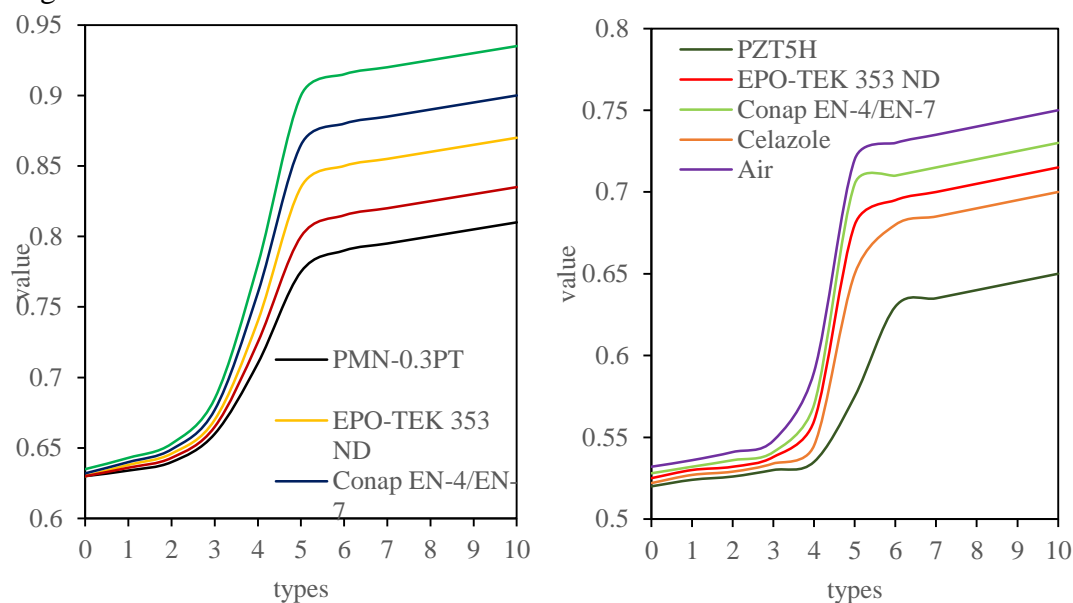


Figure 6. The dependence of PZT5H and PMN-0.3PT units with different filling materials on G

As the ratio G increases, the electromechanical coupling coefficient of the piezoelectric column increases, and finally reaches saturation. When $G > 1$, the effect of the stiffness coefficient of the filling material on the electromechanical coupling coefficient increases, while when $G < 1$, there is almost no effect. And as the stiffness coefficient of the filling material decreases, the saturation value of the electromechanical coupling coefficient of the piezoelectric column increases. For

example, when the filling material is air, with the increase of the G value, the saturation value of PZT-5H ceramic and PMN-0.3PT single crystal is the k33 value of the ceramic pillar and the longitudinal k33 of the single crystal pillar, which are 0.75 and 0.92, respectively. This result also verifies the correctness of the model from the side.

3.2. ANSYS Performance Analysis of Ultrasonic Diagnostic Transducer

When designing an ultrasonic transducer, we always hope that the surface vibration displacement of the two-phase material in the composite material is the same, so the surface displacement of the two-phase material must be studied. We extracted the first-order mode shape displacements of points C and P from the ANSYS analysis results. The displacements of the two points are shown in Table 4. The displacement result here is the relative displacement calculated by ANSYS, not the actual displacement.

Table 4. Displacement of point C and point P

Aspect ratio	V=0.2		V=0.4		V=0.6		V=0.8	
	C	P	C	P	C	P	C	P
0.1	4680.01	3799.8	5300.2	4590.12	5520.2	4999.97	5619.8	5301.02
0.2	2439.88	1500.8	2670.01	2009.85	2780.12	2250.6	2819.9	2451.11
0.3	1720.12	690.03	1799.58	1129.8	1900.6	1320.3	1900.2	1490.2
0.4	1349.86	31.02	1400.2	649.89	1409.8	839.67	1429.98	1002.6
0.5	1059.89	-399.87	1109.9	300.6	1139.9	540.06	1160.2	679.8
0.6	670.5	-429.98	899.9	1.98	959.8	309.98	979.9	459.96
0.7	370.1	-229.97	500.01	-140.2	799.68	120.1	860.9	289.99
0.8	219.98	-120.3	249.99	-120.3	379.98	38.02	649.89	120.06

The curve of the displacement consistency with the width-to-thickness ratio and the volume fraction of the piezoelectric phase shown in Figure 7, and the ordinate represent the P displacement and C displacement. As the aspect ratio increases, the inconsistency of displacement becomes more and more serious. The low piezoelectric phase volume fraction of the composite material is the most obvious. With the increase of the aspect ratio, the piezoelectric phase volume fraction of the composite material of 20% and 40%, the vibration direction of the two points is the same and becomes the opposite. This is because when the composite material undergoes thickness vibration, the piezoelectric column or polymer will expand laterally, which will cause the other phase to contract laterally. Therefore, the above situation will occur when thickness vibration occurs.

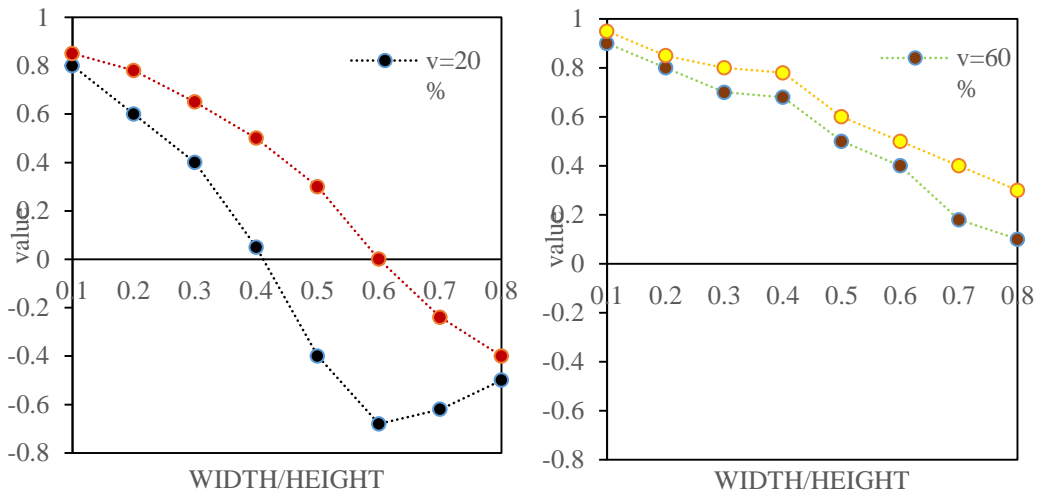


Figure 7. The curve of displacement consistency with width-to-thickness ratio

The curves of resonance frequency and anti-resonance frequency with width-to-thickness ratio are shown in Figure 8. It can be seen from the left picture of Fig. 8 that the composite material with high voltage electric phase volume fraction is less affected by the aspect ratio. When the aspect ratio is increased from 0.2 to 0.8, the resonant frequency of the composite material of 80% by volume is reduced by 8%; the resonant frequency of the composite material of 60% by volume is reduced by 14%. For composite materials with low piezoelectric phase volume fraction, when the aspect ratio is greater than 0.4, the resonance frequency changes greatly. With the increase of the aspect ratio, the resonant frequency of the composite material of 40% by volume is reduced by 24%; the resonant frequency of the composite material of 20% by volume is reduced by 34%.

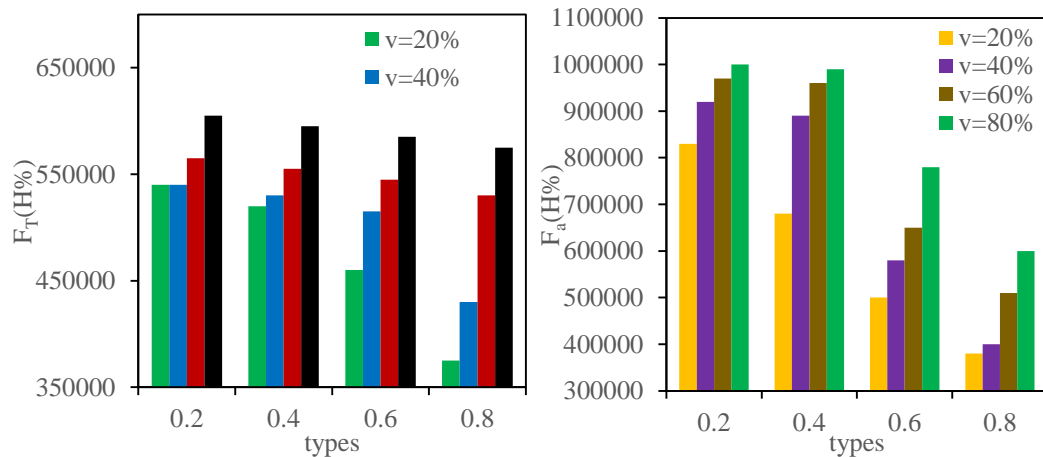


Figure 8. Frequency vs. width-to-thickness ratio

It can be seen from the right figure of Figure 8 that when the composite material with a larger volume fraction of the piezoelectric phase has an aspect ratio less than 0.4, the anti-resonant frequency is almost not affected by the aspect ratio. When the aspect ratio is greater than 0.4, the anti-resonant frequency decreases rapidly. The aspect ratio is increased to 0.8, the anti-resonant frequency of 80% by volume is reduced by 43%; the anti-resonant frequency of 60% by volume is reduced by 48%; for composite materials with a smaller piezoelectric phase volume fraction, as the

aspect ratio increases, the anti-resonant frequency gradually decreases, the anti-resonant frequency of 40% by volume is reduced by 55%, and the anti-resonant frequency of 20% by volume is reduced by 56 %.

The relationship between the longitudinal wave velocity and the width-to-thickness ratio of the 1-3 piezoelectric composite is shown in Figure 9. When the thickness is constant, as the aspect ratio increases, the change of the longitudinal wave velocity is consistent with the change of the resonance frequency.

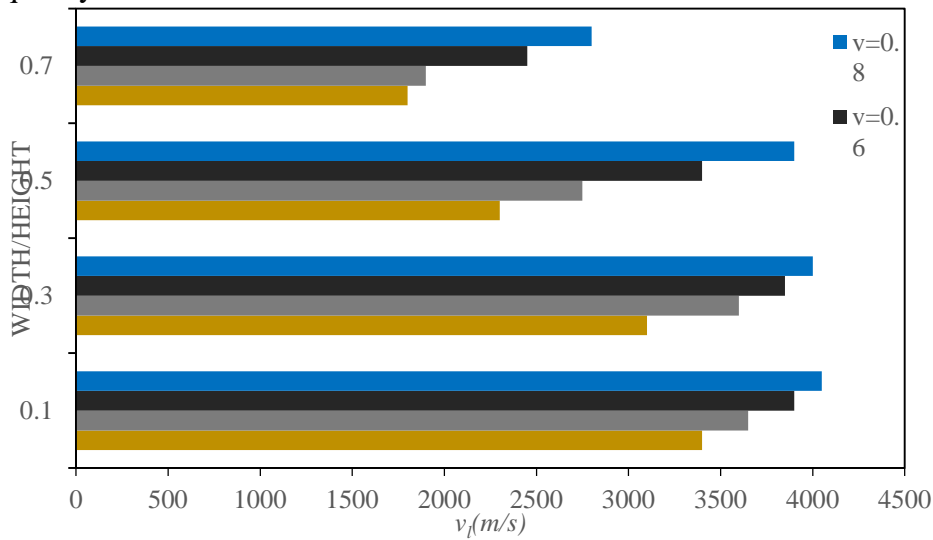


Figure 9. Graph of longitudinal wave velocity versus width-to-thickness ratio

The curve of thickness electromechanical coupling coefficient with width-thickness ratio is shown in Figure 10.

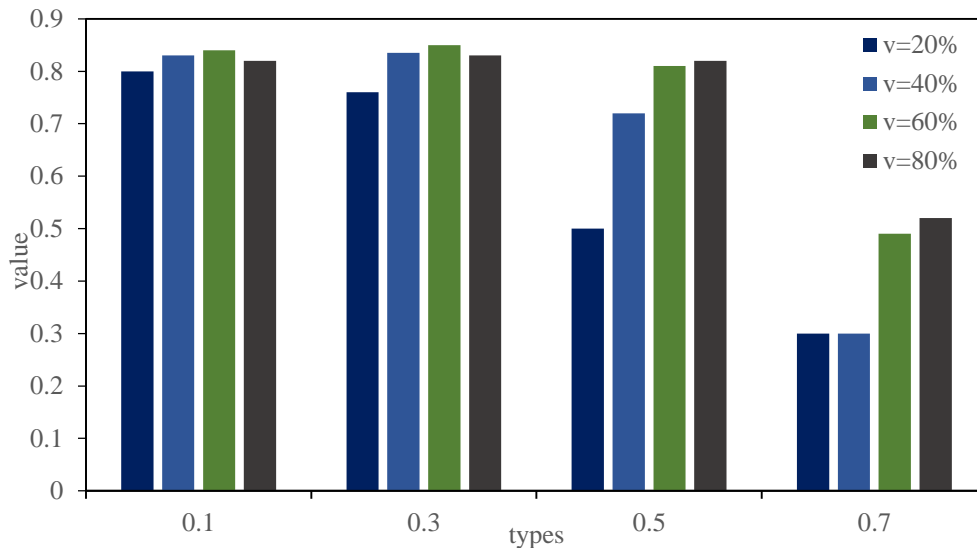


Figure 10. Thickness electromechanical coupling coefficient changes with width-thickness ratio

When the width to thickness ratio of the composite material is less than 0.4, the thickness electromechanical coupling coefficient is less affected by the aspect ratio. However, when the aspect ratio is greater than 0.4, the thickness electromechanical coupling coefficient decreases

rapidly. When the aspect ratio is increased to 0.7, the electromechanical coupling coefficient of the thickness with a volume fraction of 80% is reduced by 79%. The electromechanical coupling coefficient of the thickness with a volume fraction of 60% is reduced by 73%, and the electromechanical coupling coefficient of the thickness with a volume fraction of 20% is reduced by 68%.

4. Discuss

Piezoelectric ultrasonic transducers use piezoelectric materials with piezoelectric effects, such as quartz pulses, piezoelectric ceramics, and piezoelectric coatings to perform cross-conversion between photoelectric signals and acoustic information. And perform cross-conversion of sound energy. In some specific application areas such as medical ultrasound, underwater acoustics and industrial non-destructive testing, the transducer is required to have the characteristics of broadband, narrow pulse and high sensitivity at the same time. The corresponding piezoelectric materials also need to have both the acoustic impedance matching the easy load and the efficient mechanical coupling coefficient. However, the general single-phase fault piezoelectric sensing material has large acoustic impedance and cannot match the load range. In order to overcome the above-mentioned shortcomings of traditional piezoelectric materials, people are committed to the research of new piezoelectric materials. The piezoelectric sensing composite material made of single-phase piezoelectric material and polymer material produced in the 1970s made up for the defects of a single piezoelectric material and maintained the high-voltage electrical properties of a single piezoelectric material. At the same time, it has lower acoustic impedance and more electromechanical coupling coefficient, which is suitable for manufacturing high-sensitivity, wide-frequency, narrow pulse circuit transducers. Since the advent of piezoelectric composite materials, they have been widely used as basic building materials for piezoelectric ultrasonic transducers in many fields. Among the many piezoelectric composite materials, 1-3 piezoelectric composite materials are the most in-depth and most commonly used type of piezoelectric composite materials. It is a kind of composite composed of one-dimensional connected piezoelectric materials arranged in parallel in a three-dimensional connected polymer matrix.

5. Conclusion

The 1-3 piezoelectric sensing composite material has many advantages such as low acoustic impedance, low dielectric constant, and large thickness mechanical coupling coefficient. It has been widely used in the fields of ultrasonic transducer, non-destructive measurement, biomedical imaging and so on. Type 1-3 piezoelectric composites are composed of two-phase materials, and their performance is related to many factors. This article focuses on the various factors that affect the performance of 1-3 type piezoelectric composites. The ANSYS system performance analysis was carried out on the characteristics of the 1-3 piezoelectric composite material, and the following results were obtained: the thickness electromechanical coupling coefficient of the 1-3 piezoelectric composite material is affected by the thickness electromechanical coupling coefficient of the piezoelectric phase material, the volume fraction of the piezoelectric phase, and the width-to-thickness ratio. The greater the thickness electromechanical coupling coefficient of the piezoelectric phase material, the greater the thickness electromechanical coupling coefficient of the composite material. The piezoelectric phase volume fraction is less than 30%, and the thickness electromechanical coupling coefficient gradually becomes larger; when the piezoelectric phase volume fraction is within the range of 30%-80%, the electromechanical coupling coefficient

changes little, and the thickness electromechanical coupling coefficient is the largest at about 60% ; when the piezoelectric phase volume fraction is greater than 80%, the thickness electromechanical coupling coefficient gradually decreases. The thickness electromechanical coupling coefficient is also affected by the aspect ratio. The smaller the volume fraction of the piezoelectric phase and the larger the aspect ratio, the more the thickness of the electromechanical coupling coefficient decreases. On the contrary, the impact is smaller.

Funding

This article is not supported by any foundation.

Data Availability

Data sharing is not applicable to this article as no new data were created or analysed in this study.

Conflict of Interest

The author states that this article has no conflict of interest.

References

- [1] Dudley N J , Woolley D J . An adaptation of the ultrasound transducer element test for multi-row arrays . *Physica Medica*, 2021, 84(9):109-115. <https://doi.org/10.1016/j.ejmp.2021.04.008>
- [2] Westerway S C, Basseal J M. Advancing infection control in Australasian medical ultrasound practice . *Australasian Journal of Ultrasound in Medicine*, 2017, 20(1):26–29. <https://doi.org/10.1002/ajum.12046>
- [3] Hager P A, Bartolini A, Benini L. Ekho: A 30.3W, 10k-Channel Fully Digital Integrated 3-D Beamformer for Medical Ultrasound Imaging Achieving 298M Focal Points per Second . *IEEE Transactions on Very Large Scale Integration Systems*, 2016, 24(5):1936-1949.
- [4] Lee W, Roh Y. Ultrasonic transducers for medical diagnostic imaging . *Biomedical Engineering Letters*, 2017, 53(2):1-7.
- [5] Lei M, Landis C. The Impact of Composite Effect on Dielectric Constant and Tunability in Ferroelectric–Dielectric System . *Journal of the American Ceramic Society*, 2016, 99(11):3818-3820. <https://doi.org/10.1111/jace.14415>
- [6] Wang D, R Melnik, Wang L. Material influence in newly proposed ferroelectric energy harvesters . *Journal of Intelligent Material Systems & Structures*, 2018, 29(16):3305-3316. <https://doi.org/10.1177/1045389X18783092>
- [7] Lange S, Ricoeur A. Modeling the constitutive behavior of ferroelectric, ferromagnetic and multiferroic materials by using the condensed method (CM) . *Pamm*, 2016, 16(1):463-464.
- [8] Avakian A, Ricoeur A. Constitutive modeling of ferromagnetic and ferroelectric behaviors and application to multiferroic composites . *Pamm*, 2016, 16(1):423-424.
- [9] Labusch M, Schroeder J, Lupascu D C. A two-scale homogenization analysis of porous magneto-electric two-phase composites . *Archive of Applied Mechanics*, 2019, 89(6):1123-1140.
- [10] Yu H, Zhang J, Wei M, et al. Enhanced energy storage density performance in (Pb 0.97 La 0.02)(Zr 0.5 Sn 0.44 Ti 0.06)–BiYO 3 anti-ferroelectric composite ceramics . *Journal of*

- Materials Science: Materials in Electronics*, 2017, 28(1):832-838. <https://doi.org/10.1007/s10854-016-5597-8>
- [11] Want B, Rather M, Samad R. Dielectric, ferroelectric and magnetic behavior of BaTiO₃–BaFe₁₂O₁₉ composite . *Journal of Materials Science Materials in Electronics*, 2016, 27(6):5860-5866. <https://doi.org/10.1007/s10854-016-4503-8>
- [12] Karzova M M, Yuldashev P V, Rosnitskiy P B, et al. Numerical approaches to simulating nonlinear ultrasound fields generated by diagnostic-type transducers . *Bulletin of the Russian Academy of Sciences Physics*, 2017, 81(8):927-931. <https://doi.org/10.3103/S1062873817080135>
- [13] Louie G. PNW learns about medical ultrasound . *Journal of the Audio Engineering Society*, 2016, 64(10):816-816.
- [14] Eriksson T, Ramadas S N, Dixon S M. Experimental and simulation characterisation of flexural vibration modes in unimorph ultrasound transducers . *Ultrasonics*, 2016, 65(5):242-248.
- [15] Grynevych A A , Loboda V V. An electroded electrically and magnetically charged interface crack in a piezoelectric/piezomagnetic bimaterial . *Acta Mechanica*, 2016, 227(10):1-19.
- [16] Guo S J, Yang C H, Jiang X M, et al. High ferroelectric performance of Bi_{0.9}La_{0.1}FeO₃ thick film by optimizing preparation precursor solution . *Journal of Sol-Gel Science and Technology*, 2016, 80(1):1-6. <https://doi.org/10.1007/s10971-016-4059-3>
- [17] Sui Y, Chen W T, Ma J J, et al. Dielectric and Piezoelectric Properties of 0-3 PZT/PVDF Composite Doped with Polyaniline . *Journal of Wuhan University of Technology*, 2016, 6(9):7364-7369.
- [18] Dan Y, Zhao M, Wang C, et al. Amorphous phases and composition dependence of piezoelectricity in BaTiO₃–Bi₂O₃ polar amorphous ceramics . *Ceramics International*, 2016, 42(1):1777-1781.
- [19] Han H S, Heo D J, Dinh T H, et al. The effect of high-energy ball milling on the electromechanical strain properties of Bi-based lead-free relaxor matrix ferroelectric composite ceramics . *Ceramics International*, 2017, 43(10):7516-7521.
- [20] Mahato D K, Molak A, Szeremeta A Z. Relaxations in Doped PZT and Epoxy-glue/Bi-Mn-O Composite . *Materials Today Proceedings*, 2017, 4(4):5488-5496.
- [21] Xu X J, Deng Z C, Zhang K, et al. Surface effects on the bending, buckling and free vibration analysis of magneto-electro-elastic beams . *Acta Mechanica*, 2016, 227(6):1557-1573. <https://doi.org/10.1007/s00707-016-1568-7>
- [22] Rianyoi R, Potong R, Ngamjarurojana A, et al. Mechanical, dielectric, ferroelectric and piezoelectric properties of 0–3 connectivity lead-free piezoelectric ceramic 0.94Bi_{0.5}Na_{0.5}TiO₃–0.06BaTiO₃/Portland cement composites . *Journal of Materials Science: Materials in Electronics*, 2021, 32(4):4695-4704.
- [23] Gherrous M, Ferdjani H. Analysis of a Griffith crack at the interface of two piezoelectric materials under anti-plane loading . *Continuum Mechanics and Thermodynamics*, 2016, 28(6):1-22. <https://doi.org/10.1007/s00161-016-0501-6>
- [24] Tang Q, Zhen T, Danyun L I, et al. Mechanical Properties of Graphene/Hydroxyapatite Composite Materials:Numerical Study . *Jisuan Wuli/Chinese Journal of Computational Physics*, 2018, 35(1):71-76.
- [25] Azab A A, El-Khawas E H, Abdellatif M H. Enhancing the Ferroelectric Coupling of Multifunctional Spinel–Perovskite Composite . *Journal of Electronic Materials*, 2019, 48(10):6460-6469. <https://doi.org/10.1007/s11664-019-07434-w>